NACA RM E56C06

NACA

RESEARCH MEMORANDUM

FABRICATION TECHNIQUES AND HEAT-TRANSFER RESULTS FOR CAST-CORED AIR-COOLED TURBINE BLADES

By John C. Freche and Robert E. Oldrieve

Lewis Flight Propulsion Laboratory
Cleveland, Ohio

NATIONAL ADVISORY COMMITTEE
FOR AERONAUTICS
WASHINGTON

June 22, 1956
Declassified December 13, 1957

ERRATA

NACA RESEARCH MEMORANDUM E56C06

By John C. Freche and Robert E. Oldrieve

1956

Page 3, paragraph 3: Lines 4 to 6 should read "for 48 hours. Excess moisture was poured off and after a 12-hour drying period, the investment mold was placed in a furnace to melt out the wax pattern. The furnace was at room temperature when the mold was inserted. The furnace temperature was then raised to 220° F and maintained at this value for 18 hours. (The hold for 18 hr at 220° F is not a general requirement.) This temperature" . . .

Page 4, paragraph 1, lines 2, 8, and 16. Delete "solution."

Issued 9-5-58

NACA - Langley Field, Va.

NATIONAL ADVISORY COMMITTEE FOR AERONAUTICS

RESEARCH MEMORANDUM

FABRICATION TECHNIQUES AND HEAT-TRANSFER RESULTS FOR CAST-CORED AIR-COOLED TURBINE BLADES

By John C. Freche and Robert E. Oldrieve

SUMMARY

An investigation was conducted to devise an air-cooled turbine blade which eliminated the difficulties encountered with brazing in air-cooled-blade fabrication. Techniques were developed for casting air-cooled blades with a large number of relatively small cooling passages near the airfoil surface; two such blades of HS-21 material were operated in a turbojet engine modified for air cooling.

Heat-transfer data obtained at rated engine operating conditions indicated that substantial reductions from the effective gas temperature occurred in the central portion of the highly stressed root region. At a coolant-to-gas flow ratio of 0.010, the temperature of this region was 760° F, a 520° F reduction from effective gas temperature.

One of the two test blades was operated without failure for 78 hours at a centrifugal blade stress of 42,150 pounds per square inch based on total metal area at the blade root at rated engine speed and an average inlet gas temperature of 1735° F. Of this total, 50 hours were obtained with an average blade root metal temperature of 883° F (coolant-to-gas flow ratio, 0.015), and 28 hours with an average blade root metal temperature of 1130° F (coolant-to-gas flow ratio, 0.004). Calculations indicate that a flow ratio of approximately 0.023 is required to maintain an average root temperature of 883° F in the application of this blade to a turbojet engine at a Mach number of 2, an altitude of 50,000 feet, and an inlet gas temperature of 2000° F.

INTRODUCTION

Air-cooled turbine rotor blades have been under investigation at the NACA Lewis laboratory for several years. The results of cooling and/or endurance performance of various cooled turbine rotor-blade configurations are reported in references 1 to 12. Brazing was primarily employed in the assembly process of these blades. In order to eliminate the brazing problems encountered, an investigation was undertaken with a blade having an all-cast structure.

Earlier investigations (refs. 1 to 8) employed blades that generally were assembled from three main components consisting of a cast base, a formed hollow shell, and tubes or fins inserted into the hollow shell to increase the coolant heat-transfer surface area. The tube or fin inserts were brazed into the blade shell. The details of the fabrication methods for these blades are given in references 11 and 13.

A detailed endurance investigation of shell-supported-type turbine blades made from a noncritical material and utilizing the three-piece brazed-component-type fabrication method indicated that the brazing process can cause chemical attack on the parent metal, grain growth in the shell adjacent to the brazed area, and undercutting of the shell (ref. 11). Such effects can seriously reduce the strength and ductility of the metal in the brazed region. An endurance study of strut-supported-type air-cooled turbine blades made from high-temperature alloys brazed together shows similar results (ref. 12). The detrimental effects of brazing the blades used in these investigations were generally concentrated in the highly stressed root region of the blade and often were the cause of early blade failure or erratic blade life. These brazing problems can generally be greatly minimized by carefully controlling the brazing process and applying suitable heat treatment to the blade after brazing.

In order to provide an alternate method of cooled-blade fabrication which may be more suited to the facilities of some manufacturers, an air-cooled-blade configuration was evolved in which large numbers of small coolant passages were cast near the surface of the airfoil. This configuration will be referred to herein as a cast-cored blade. A similar attempt was made in reference 14; however, only partial success was achieved in removing ceramic cores from the final casting.

The base and airfoil of the blade discussed herein were cast integrally from HS-21, a high-temperature alloy. This report presents (1) the fabrication techniques developed, (2) the experimental cooling results obtained with this blade configuration, (3) a comparison of these results with other air-cooled blade data, and (4) preliminary endurance results.

The cast-cored turbine blades were operated at sea-level ambient conditions in a turbojet engine modified to accommodate two air-cooled blades. Heat-transfer data were obtained over a range of cooling-air flows at several constant engine speeds from 4,160 to 11,500 rpm (rated speed). The centrifugal blade stress based on total metal area at the base was 42,150 pounds per square inch at rated engine speed. The ratios of coolant-to-gas flow ranged from 0.008 to 0.045. A preliminary endurance evaluation of the blade configuration was made at an engine speed of 11,500 rpm, an average turbine-inlet gas temperature of 1735° F, and coolant-to-gas flow ratios of 0.015 and 0.004.

BLADE FABRICATION

Steps in Casting Process

Precision investment casting by the lost-wax process was the fabrication method employed. A wax pattern was prepared in precision dies by first placing two strips of pattern wax, approximately 3/8 inch wide by 0.030 inch thick, in each precision die half. Then, commercially available hollow ceramic cores (mullite) were laid adjacent to each other and lightly pressed into the wax strips as shown in figure 1. Cores having outside diameters of approximately 0.060 and 0.040 inch were used in the blades investigated. Six 0.040-inch-diameter cores were used in the blade trailing-edge region; thirty-four 0.060-inch-diameter cores were used for the rest of the blade. The inside diameter of all the ceramic cores was 0.020 inch. Although not shown in the core assembly (fig. 1), adjacent cores were tied to each other by Nichrome wire at several spanwise stations to form attached pairs, thus providing additional core stability during casting. X-ray inspection of the final castings revealed several irregularities caused by partial melting of these wires. The spacing between adjacent pairs of cores was approximately 0.040 inch. In order to achieve sufficient core strength without wiring, oval-shaped cores with a major-axis diameter roughly equivalent to twice the round-core diameter may be used. However, these cores were not immediately available during this investigation.

The next step in the fabrication procedure was to join the two halves of the die and fill the blade cavity with molten wax under pressure. Upon hardening, the completed wax pattern was removed from the die and attached to a wax sprue (fig. 2). The dark area along the blade trailing edge results from use of a patching wax to fill in surface imperfections. Several 0.009-inch Nichrome wires extend from the wax pattern shown in figure 2. These wires were wrapped around individual cores, and the exposed ends were embedded in the investment material, thus serving as additional core anchors. The problem of irregularities in the final casting due to these wires is not severe, because only a few anchor wires are needed, usually for the small-diameter cores near the trailing edge.

The wax pattern was next invested in a flask using silica with a commercial binder as the investment material. After removing air from the investment in a vacuum chamber, the investment was allowed to settle for 48 hours. Excess moisture was poured off and after another 12-hour drying period, the investment was placed in a furnace to melt out the wax pattern. A furnace temperature of 220° F was maintained for 18 hours. This temperature was then advanced at the rate of 100° F per hour until 1800° F was reached in order to remove all wax traces, to cure, and to heat the mold prior to pouring. The investment, still in its flask, was next placed in a centrifugal casting machine and inverted above a crucible

of molten metal. (The base and airfoil of the blade were cast integrally from HS-21.) Upon locking the investment mold to the crucible, the casting machine was put in motion. The investment mold was rotated with the blade leading edge forward in order to minimize bowing of the ceramic cores. After approximately 5 minutes of rotation at 130 rpm, casting was complete.

Removal of Ceramic Cores From Casting

Ceramic cores were removed from the cast HS-21 blade by means of the chemical reaction between molten sodium hydroxide solution and the ceramic. Simple immersion was not successful, since only the core portions near the blade tip and root were exposed to the solution. Insertion of the liquid sodium hydroxide under pressure was not attempted because of its complexity and the unfavorable results obtained with this method (ref. 14). Consequently, a device was constructed which permitted exposure of the ceramic cores to the sodium hydroxide solution along the entire blade length (fig. 3). Stainless-steel wires were threaded through each of the hollow ceramic cores in the blade. These wires were then firmly attached at each end to a blade support structure which was partially immersed in molten sodium hydroxide. A connecting rod, spot-welded to the blade base, was joined to a gear system powered by an electric motor. Rotative motion of the motor was transferred through the gears to reciprocal motion of the blade along the stainless-steel wires. The wires were also immersed in the sodium hydroxide solution along a portion of their length. Reciprocal motion of the blade along these wires scraped away the parts of the ceramic cores attacked by the sodium hydroxide, thus exposing a fresh surface to chemical action until the entire core was removed. Although only one blade support structure is shown in figure 3, there is provision for attaching four to the mounting bracket. The core removal process, which required 2 hours, was successful.

Additional Fabrication Steps

In order to reduce blade root stress and blade weight, material was removed from the upper portion of the blade by electrical disintegration. Figure 4 shows the void at the blade tip. This metal may also be removed during the casting process by providing a suitable coring arrangement. In the present investigation, electrical disintegration was employed in order to simplify the casting development program. Electrical disintegration rather than drilling was used because of the relatively poor machinability of the blade material.

The blades described herein were among the first castings obtained by this process, and shrinkage cracks occurred in the upper surface of the base and extended into the fillet. This condition was remedied in subsequent casts. In order to determine if crack propagation could be retarded by filling the cracks, a thin film of Nicrobraz with a cement

binder was painted over the base region of one of the blades, and the blade was put through a brazing cycle. Neither of the two blades cast was subjected to a heat-treat cycle. Serrations were ground into the blade bases prior to blade instrumentation.

APPARATUS AND INSTRUMENTATION

Air-Cooled Turbine Blades

The air-cooled blades used in this investigation had a span of 4 inches and a chord of 2 inches. The airfoil was tapered from root to tip in order to obtain suitable centrifugal-stress levels within the airfoil material, and the blade was twisted from root to tip. Thirty-four 0.060-inch coolant passages and six 0.040-inch coolant passages were provided. Essentially, the passages formed two rows, one following the contour of the pressure surface and the other following the contour of the suction surface. The void shown in the central portion of the blade at the tip (fig. 4) was for the purpose of reducing weight. The cross-sectional areas of the blades were greater than those of the standard uncooled blades for this engine at all spanwise positions above the blade base. The profiles and cross-sectional areas at the hub of the research blades were the same as those of the standard blades. The exaggerated airfoil thicknesses resulted primarily from use of the same casting dies previously employed for making hollow air-cooled blades for this engine and partly from use of patching wax as discussed previously.

Engine Modifications

The engine modifications are described in detail in reference 1. Blade cooling air was provided from an external source (laboratory service air system) and was ducted to the test blades through two tubes fastened to the rotor rear face and through passages drilled transversely through the rotor rim beneath the test blades. The two cooled test blades were located diametrically opposite each other in the rotor. The rotor assembly was completed with 52 standard S-816 blades. The engine was equipped with an adjustable tailpipe nozzle so that the turbine-inlet temperature could be varied at a given engine speed.

Blade Instrumentation

Blade thermocouple locations are shown in figure 5. Four chromel-alumel thermocouples were installed on one of the cooled blades and three on the other. Six of these thermocouples were embedded immediately below the blade surface. The seventh was installed in the central portion of the blade root section. Two standard blades (reference blades) were each

provided with one thermocouple at the leading edge, approximately at the 1/3-span position. The reference blades were cut off at the 2/3-span position to reduce centrifugal stress.

Engine Instrumentation

Engine speed, air flow, fuel flow, cooling-air flow and temperature, and tailpipe gas temperature were all measured as described in reference 1.

PROCEDURE

Heat-Transfer Investigation

The cast-cored blade-cooling effectiveness was determined in a manner similar to that described in reference 1. Blade temperature data were obtained over a range of engine speeds from 4,160 to 11,500 rpm (rated) and over a range of effective gas temperatures from 1124° to 1488° F. At each engine speed the coolant-to-gas flow ratio (hereinafter called coolant-flow ratio) was varied. Since the rated engine speed data are of major interest, these alone are reported. The coolant-flow-ratio range covered at rated speed was from 0.008 to 0.045. These values took into account the quantity of coolant leakage between the rotating and stationary parts of the cooling-air system as determined by a separate calibration.

Blade Durability Investigation

The durability of the cast-cored blade with the base coating of Nicrobraz was investigated by rated speed operation (11,500 rpm) at two coolant-flow ratios, 0.015 and 0.004, after completion of the heat-transfer investigation. An average inlet gas temperature of 1735° F was maintained, although mechanical difficulties with the adjustable exhaust nozzle resulted in brief operating periods at a minimum gas temperature of approximately 1680° F and a maximum of approximately 1790° F. After 50 hours of operation at the higher coolant-flow ratio, operation was continued at the lower flow ratio. The lower coolant-flow ratio (0.004) was selected for additional endurance operation, because it represented the lowest coolant flow that could be accurately maintained in this installation. The significance of this endurance operation will be discussed in a subsequent section.

Prior to installation in the engine, the test blade was inspected by X-ray and zyglo inspection methods. At convenient intervals during endurance operation, the engine was shut down and the test blade was inspected by the zyglo method to determine if cracks were developing.

Cooling-Air-Leakage Calibration

As in previous investigations, cooling-air leaks occurred through the labyrinth seal between the stationary cooling-air supply tube and the pilot-bearing housing in the rotor hub (fig. 3, ref. 1). Consequently, a calibration was made over the entire coolant-flow range investigated (as in ref. 11) to determine the quantity of leakage across this junction.

CALCULATIONS

Heat-Transfer Calculations

Average blade surface temperature. - The average blade surface temperature at two spanwise positions (root and 1/3 span) was calculated from the following equation to facilitate comparisons with other air-cooled blade configurations:

$$\overline{T}_{B,l} = \overline{T}_{g,e} - \frac{\frac{\overline{\Delta T}_a}{\Delta z} - \frac{\omega^2}{Jgc_{p,a}}\left(r_r + z - \frac{\Delta z}{2}\right)}{\frac{\overline{h}_o l_o}{w_a c_{p,a}}} \qquad (1)$$

(All symbols are defined in the appendix.) This is equation (D2) of reference 15 expressed in slightly different form. Essentially, the previous expression is a finite-difference equation for the cooling-air temperature rise as it passes through the blade, since the blade temperature is dependent upon the cooling-air temperature at a given spanwise position. Equation (1) is applicable to the case where the effective gas temperature, as well as the product of the gas-to-blade heat-transfer coefficient and the outside blade perimeter, vary along the span. A constant spanwise value of $\overline{h}_o$ and local spanwise values of $T_{g,e}$ were used. For the engine employed in this investigation, the gas temperature profile at the turbine inlet was approximately parabolic from root to tip. Since blade temperatures at the root region were calculated, it was desirable to take the large spanwise gas temperature variation into account. The gas-to-blade heat-transfer coefficient for this blade profile at the blade design conditions was theoretically determined. Blade velocity profiles were obtained from stream-filament theory as described in reference 16 and were used to obtain the heat-transfer coefficient by the method of reference 17.

Blade-to-coolant heat-transfer coefficients used in the iterative process in determining ΔT_a were obtained from a heat-transfer correlation

expressing the flow of air through stationary ducts. This correlation is given in reference 18. The calculated average surface blade temperatures at the root were then compared with integrated average experimental values obtained at the same station over a range of coolant-flow ratios.

The procedure described does not consider the effect of conduction to the rotor rim. These effects are not included because the calculation procedure involved is tedious and time consuming.

Blade trailing-edge temperatures. - Sufficient thermocouples were not available at the blade tip to provide an average experimental tip temperature for comparison with calculated values. One thermocouple was provided at the tip trailing edge (fig. 5), however, and the temperature at this location was calculated. The one-dimensional method described in reference 19 was employed. The blade trailing-edge section was approximated by a rectangle and the temperature-distribution equation

$$\theta = \frac{\frac{h_i}{k_B}(T_{g,e} - T_a)\cosh(\varphi y')}{\varphi \sinh \varphi j' + \frac{h_i}{k_B}\cosh \varphi j'} \qquad (2)$$

(eq. (19) of ref. 19) was used. Constant spanwise values of the gas-to-blade heat-transfer coefficient and the blade-to-coolant heat-transfer coefficient (both obtained as described in the section "Average blade surface temperatures") were used. Tip cooling-air temperatures were used in equation (2) and were determined by equation (1). Again, local $T_{g,e}$ values were employed. Equation (2) was also used to calculate the root trailing-edge temperature, and also neglects conduction effects.

Stress Calculations

Blade allowable-to-centrifugal-stress ratio. - The cast-cored blade presents a unique stress situation. The double row of coolant passages in the cast-cored blade tend to separate it into a relatively cool central region and a higher-temperature outer region (area between coolant passages and blade surface). Consequently, thermal stresses are set up which place the central region in tension and the outer region in compression. As a result, if the coolant passages are located too close together, shear failure could result in the region between adjacent passages. The 0.040-inch spacing employed in this case is apparently satisfactory, at least for limited periods of operation, as endurance results show. Since the blades did not fail in this region and since evaluation of the thermal stresses described is a complex procedure, the evaluation was not attempted.

The controlling blade stress was considered to be the centrifugal stress based upon total metal area at the spanwise position considered. Calculations were made for both root and 1/3-span positions in order to establish limits, which would probably include the blade critical section. Use of the total metal cross-sectional area assumes that deformation is uniform over the blade cross section, a clearly optimistic assumption in view of the temperature differences discussed previously. A more pessimistic assumption would be that the entire centrifugal load is supported only by the central metal area enclosed by the two rows of coolant passages. Sample calculations made in this manner indicated that the root centrifugal stress was above the ultimate strength of the blade material, and this procedure was abandoned as being overly pessimistic.

The allowable blade stress was determined from the average blade temperature at the spanwise station considered and stress-to-rupture or yield-strength data, whichever was applicable, for the blade material (cast HS-21). For the root station, an average of experimentally obtained blade temperatures was employed. This average was weighted on an area basis to account for the area difference between the blade central portion and the region between the coolant passages and the blade surface. Since no experimentally obtained temperatures were available, calculated values were used at the 1/3-span position. The same relation that existed between the blade central-portion temperature and the surface temperature at the root was assumed to exist at the 1/3-span position, and an average metal temperature also weighted on an area basis was obtained.

RESULTS AND DISCUSSION

Heat-Transfer Results

Experimental blade temperature distributions. - The change in blade temperature with coolant-flow ratio at rated engine operating conditions for each of the thermocouple blade stations is shown in figure 6. The effective gas temperature (uncooled-blade temperature) at each spanwise station is included. Root and tip effective gas temperatures were obtained from unpublished NACA data, which provided effective gas temperature profiles for this engine at corresponding tailpipe-nozzle settings and engine speeds. Failure of one of the blades and of several thermocouples resulted in lack of temperature data at most stations for coolant-flow ratios above 0.023. The cooling-air temperature measured at the blade base entrance in the rotor rim varied from 340° F at a coolant-flow ratio of 0.008 to 215° F at a coolant-flow ratio of 0.023.

At a coolant-flow ratio of 0.010, surface temperatures at the highly stressed blade root were lower than the effective gas temperature by 80° F at the leading and trailing edge and by 280° F at the midchord region. Greater reductions in leading- and trailing-edge temperatures probably

can be expected with this type blade by using oval-shaped ceramic cores to form the leading- and trailing-edge passages. Such cores may be fitted more readily into these narrow blade sections and thereby reduce the length of the uncooled regions. In the central portion of the blade at the root section, which represents a large part of the blade stress-supporting area, the temperature should be relatively low in order to provide adequate metal strength. A 520° F reduction from effective gas temperature occurred in this region at a flow ratio of 0.010. It should be noted, however, that low temperatures in the blade central region accompanied by high surface temperatures can result in unfavorable thermal stresses. Consequently, the coolant passages should be carefully located to minimize blade hot spots.

Comparison of calculated and experimental blade temperatures. - A comparison of calculated and experimental blade temperatures is shown in figure 7 at rated speed and a turbine-inlet gas temperature of 1725° F over a coolant-flow-ratio range from 0.008 to 0.023. Calculated average blade root surface temperatures and average root experimental surface temperatures are compared in figure 7(a). The maximum deviation of calculated data from experimental data was 130° F and occurred at an experimental temperature of 930° F, representing a maximum error of 14 percent. All other calculated points show deviations from experimental data of less than 10 percent. Although agreement appears to be satisfactory, it should be noted that limited blade thermocouple instrumentation was employed in this investigation. Thus, it still may be necessary to correct for conduction effects in future applications.

Comparisons of calculated and experimental trailing-edge temperatures at the blade root and tip are made in figures 7(b) and (c), respectively. At the blade root the maximum deviation from the 1:1 correlation line was 70° F at an experimental blade temperature of 1130° F (approx. 6-percent error). For the blade tip the maximum deviation was 60° F at an experimental blade temperature of 1270° F (approx. 5-percent error).

Blade critical-section average temperatures. - The change in average blade temperature at rated engine speed with coolant-flow ratio is shown in figure 8. The exact critical section of the blade has not been determined; however, it probably lies between the root and 1/3-span position for the conditions of this test. The lower boundary of the temperature band extending between these spanwise stations represents the average root temperatures as determined experimentally. The upper boundary represents the 1/3-span position average temperatures calculated as described previously. Since the entire cross-sectional metal area was considered to be stress-supporting in the cast-cored blade, the averages of the surface and central-region temperatures were plotted. The band boundaries are roughly parallel, show a spread of 150° to 50° F, and decrease sharply with increasing coolant-flow ratio. The significance of these values can better be evaluated by comparison with results from other blade configurations, which will be made in the section "Temperature comparisons with other configurations."

Stress and Durability Results

Blade durability. - One of the two test blades failed at the root section after 15 hours of engine operation. Failure occurred at 11,500 rpm (root centrifugal stress, 42,150 psi) and a coolant-flow ratio of 0.008, although some of this operating time was compiled at lower speeds and other coolant-flow ratios during the heat-transfer runs. The failed blade is shown in figure 9. As stated previously, this blade had microshrink cracks in the base region resulting from casting. No attempt was made to fill the cracks in this region and these cracks are believed to have caused the premature failure.

An X-ray of this blade prior to its installation in the engine is shown in figure 10. Several Nichrome-wire inclusions are apparent. One of the cracks in the blade root region at the leading edge is also visible. Metallurgical examination of the failed blade indicated that failure was probably initiated in the region of this leading-edge crack.

Endurance operation was continued with the second test blade (base region coated with Nicrobraz) for 50 hours at rated engine speed, an average inlet gas temperature of 1735° F, and a coolant-flow ratio of 0.015. This operating condition resulted in an average root temperature of 883° F and an average root surface temperature of 1015° F. The blade root allowable-to-centrifugal-stress ratio for a life of 50 hours was 2.04. At this point, the coolant-flow ratio was lowered to 0.004, the minimum value that could be accurately maintained over long periods in this installation. The resulting average blade root temperature became 1130° F (average root surface temperature, 1185° F) providing an allowable-to-centrifugal-stress ratio of 1.6 for a life of 28 hours. Since the blade showed no sign of impending failure, operation was terminated at this time. Further reduction in the allowable-to-centrifugal-stress ratio could be achieved only by extensive operation at this condition. Zyglo inspection revealed that none of the filled-in cracks had reopened. A total of 105 hours of operating time, 78 hours of which were endurance operation at rated engine speed, was compiled with this blade. Since the blade did not fail, an actual stress-ratio factor could not be determined.

Of course, limitations of the test vehicle prevented endurance operation at higher gas temperature levels. The average blade root temperature of 883° F obtained during the actual endurance run is in a region of high metal strength properties for most turbine-blade alloys. Consequently, maintenance of this temperature would be desirable during operation at higher inlet gas temperatures. Calculations, which will be discussed more fully in the section Evaluation of Cast-Cored-Blade Potential, indicate that the required coolant-flow ratio for operation at an inlet gas temperature of 2000° F and an average root metal temperature of 883° F is not excessive, being approximately 0.023. Thus, it appears that the endurance runs conducted probably provide a realistic indication of blade potential life.

Effect of blade weight on blade stress. - One requirement for turbine-blade design is low weight in order that over-all engine weight as well as rotor-rim loading may be reduced. The reported cast-cored blade, weighing 0.82 pound, has the disadvantage of being heavier than many fabricated air-cooled-blade configurations. As a result, the blade root centrifugal stress of the cast-cored blade reported herein was 42,150 pounds per square inch at rated engine speed. This value is considerably higher than that used in current design practice. For example, the standard uncooled blade for this engine has a root-section centrifugal stress of approximately 25,000 pounds per square inch at rated engine speed. Since low root stresses are desirable in order to obtain maximum blade life, metal which does not contribute to the blade support should be eliminated. A considerable stress reduction may be effected for a cast-cored-blade configuration with rows of coolant passages along the blade contour and a large expanse of metal area bounded by these rows. In the present blade, a large part of this metal in the upper half of the blade was removed by electrical disintegration, as may be seen in figure 4. This removal resulted in a rated-speed centrifugal-stress reduction of approximately 3000 pounds per square inch from 45,150 pounds per square inch. The blade thickness and the cooling-passage location, however, will determine whether metal removal as shown herein is permissible in any specific instance.

Evaluation of Cast-Cored-Blade Potential

Temperature comparisons with other configurations. - The cast-cored blade must be compared with other air-cooled-blade configurations in order to be properly evaluated. One comparison may be made on the basis of blade temperatures and blade cooling-air pressure drop. These factors are interrelated and an independent comparison on each basis is often misleading. For example, the blade temperature comparison should probably be made at the critical section of each blade and at a constant value of blade cooling-air pressure drop. In this report the blade temperature comparison was made for the critical section of each blade but probably not at a constant value of cooling-air pressure drop. The pressure drop through individual cooling passages was not measured. For the cast-cored blade reported, the pressure drop is probably high because of the small-diameter cooling passages, particularly in the trailing-edge region. It should be noted, however, that use of larger diameter cores than those used in the blades of this investigation should reduce the pressure losses encountered. Of course, any reduction in pressure drop achieved in this manner will also reduce the heat-transfer effectiveness of the cast-cored blade. By recognizing these factors as well as the fact that, in any air-cooled blade, the coolant-passage size must be decided on the basis of a compromise between cooling requirements and pressure drop permissible for the engine application under consideration, the following temperature comparison is presented.

The change in blade temperature with coolant-flow ratio is shown in figure 11 for the cast-cored, strut, corrugated-insert, and hollow blades at the critical section of each. A temperature band extending from the root to the 1/3-span position is shown for the cast-cored blade since its exact critical section has not been determined. The blade profiles were similar at the critical section in each case, and the results were obtained in the same model test engine at turbine-inlet gas temperatures ranging from 1655° to 1725° F. The corrugation amplitude, pitch, and thickness were 0.070, 0.070, and 0.007 inch, respectively, for the corrugated-insert blade. Since the corrugated and hollow blades are of the shell-supported type, their average shell temperatures, obtained from unpublished NACA data, are plotted in figure 11. The average strut temperatures (stress-supporting member), obtained from reference 20, are plotted for the strut blade. The entire cross-sectional metal area was considered to be stress-supporting in the cast-cored blade, and, therefore, an average of the surface and central-region temperatures was plotted. Experimental data were used for the root position, and calculated values were used at the 1/3-span position for the cast-cored blade.

At coolant-flow ratios less than 0.012, the cast-cored blade temperature band encloses the corrugated- and strut-blade temperature curves (fig. 11). Above flow ratios of 0.012, the band falls between the corrugated- and strut-blade curves. Of course, the band location is subject to the accuracy of the 1/3-span temperature calculation. Over the entire flow-ratio range, the cast-cored-blade temperature band lies relatively close to the corrugated- and strut-blade temperature curves, and considerably below the hollow-blade curve (from 350° to 400° F at a flow ratio of 0.02). It should also be noted that any comparison of this type is subject to the accuracy of the cooling-air leakage calibrations. At low coolant-flow ratios in a test setup of this type, the cooling-air leakage is frequently a large percentage of the total flow. This was also the case for the installations employed to investigate the other blades in this comparison. In the low coolant-flow range, therefore, the temperature curves for all the blades may shift; however, the results shown will be qualitatively correct.

Allowable-to-centrifugal-stress-ratio comparisons. - The comparison of the cast-cored blade with the same air-cooled blade configurations at current gas temperature levels (average gas temperature, 1690° F) is continued in figure 12. This figure presents the allowable-to-centrifugal-stress ratios at the critical section for each blade plotted against coolant-flow ratio. Since the blades were of different materials, an attempt was made to provide a comparison on a common basis. The corrugated, hollow, and cast-cored blades were made of high-temperature heat-resistant alloys (N-155 and HS-21). Since thermal conductivity is about the same for each material, differences in measured blade temperatures are probably not due to material conductivity. Consequently, either the yield or stress-to-rupture properties of one of these materials (HS-21)

and the blade temperatures shown in figure 11 were used to determine the allowable stress for all blades. The centrifugal stress was also calculated for the density of HS-21 material. The strut blade was omitted from this comparison because it was of 17-22A(S) material, which has a much higher thermal conductivity than HS-21. A band is again presented for the cast-cored blade to enclose its critical section. If the critical section is assumed to fall near the 1/3-span position for the cast-cored blade, allowable-to-centrifugal-stress ratios of about 3 similar to those of the corrugated and hollow blades are obtained (fig. 12). If the critical section falls near the root, the allowable-to-centrifugal-stress ratio is nearer 2, and for a given coolant-flow ratio the margin of safety is reduced in comparison to the corrugated and hollow blades. This comparison is valid, assuming 100-hour life for each of the blades compared. Once the cast-cored blade has been run to destruction, the exact critical section will be determined and the required allowable-to-centrifugal-stress ratio, or stress-ratio factor, will be established.

Coolant-flow requirements at elevated conditions. - To further evaluate the potential of the cast-cored blade, it is desirable to know its cooling requirements in a high gas temperature, high altitude, and high flight Mach number application. A single-stage-turbine application in a turbojet engine was selected and a Mach number of 2, an inlet gas temperature of 2000° F, and a 50,000-foot altitude were specified. Analyses (ref. 21) have been made to similarly determine the cooling requirements of corrugated-insert blades at elevated conditions.

In calculating the cast-cored-blade coolant requirements, limiting surface temperatures of 1015° F at the root (average temperature, 883° F) and 1148° F at the 1/3-span position (average temperature, 995° F) were specified since reasonable blade life was obtained while maintaining these temperatures during blade durability tests. In order to obtain an indication of the validity of this calculation method, the sea-level coolant-flow ratio required for operation at these blade temperatures was calculated and compared with the experimental value. The experimental value was 0.015; the calculated value, 0.0135. The calculation was then extended to the flight conditions cited previously and a constant gas-to-blade heat-transfer coefficient (115 Btu/(hr)(sq ft)(°F)) was specified (value estimated from ref. 22). Corrected engine weight flow per unit frontal area was taken as 25.5 pounds per second per square foot. Blade cooling-air inlet temperature was considered to be 588° F (compressor-bleed temperature plus 100° F).

The calculations indicate that a coolant-flow ratio of approximately 0.019 is required to maintain the surface temperature 1148° F at the 1/3 span, while a coolant-flow ratio of approximately 0.023 would be required to maintain the root surface temperature of 1015° F. Since the blade critical section probably falls somewhere between the root and 1/3 span, these coolant-flow ratios represent the requirement limits. Both of these

values fall within the calculated coolant-flow-ratio range tabulated in reference 21 as the limitations of 80 corrugated-insert blade designs.

The corrugated-blade designs considered in reference 21 are not limited on the basis of cooling-air pressure drop. However, this may not be the case for the cast-cored blade. Thus, as in the case of the temperature comparison, the possibility of adverse pressure-drop requirements for the cast-cored blade must be noted.

Blade weight and stress considerations. - The disadvantages of the cast-cored blade reported herein from a weight and stress standpoint have already been discussed. However, in evaluating the potential of this type of blade, design variations that employ the cast-cored-blade fabrication principle should be considered. For example, this principle may be utilized in a cast-combination-type blade that has a hollow tip section (fig. 13). A sketch of such a blade is shown in figure 13(a), and a one-piece casting of this type prior to grinding the base serrations is shown in figure 13(b). The ridge along the profile in the upper part of the blade is intended to stiffen this region. The two cross members in the tip region are also stiffeners. This blade offers the advantages of reduced weight and concurrently reduced blade root and rotor-rim stress as well as a relatively favorable cooling configuration in the root region. The tip region, although not cooled as favorably, should remain intact because of the lower stresses imposed. Since the hollow tip section must support itself, a suitable taper ratio must be provided to accommodate the stress imposed at the junction between the shell and the blade lower section. The blade shown in figure 13(b) has a shell taper of 0.4 with a shell thickness of 0.013 inch at the tip. The permissible length of the hollow section must be determined by temperature and stress calculations for the particular application considered. Such calculations indicated that a hollow section approximately 45 percent of the blade span is probably satisfactory for this engine application.

The weight reduction possible with the blade illustrated in figure 13 is shown graphically in figure 14, which compares several configurations with the standard uncooled turbine blade for the engine used in this investigation. A corrugated-insert blade having corrugations with amplitude, pitch, and thickness of 0.050, 0.050, and 0.005 inch, respectively, was included. The cast-cored blade (0.82 lb) weighs 2 percent less than the standard blade, whereas the corrugated-insert blade weighs 18 percent less and the hollow blade 20 percent less. The hollow blade probably provides a minimum blade weight and rotor-rim stress for this turbine application. The figure also shows that a 13-percent weight reduction from the standard blade is possible by combining the cast-cored and hollow-blade designs as discussed previously. For convenience, the base weight was considered to be the same for the combination blade as for the cast-cored blade. A reduction in the aerodynamic profile weight would, of course, permit a reduction in base weight because of decreased root stresses. This, in turn, would permit a further slight reduction in the overall weight of the combination blade.

SUMMARY OF RESULTS

The following results were obtained from an experimental investigation of an air-cooled cast-cored turbine blade which eliminated the brazing problems encountered in fabricating some types of air-cooled blades.

1. Techniques were developed for casting an integral blade and base assembly with a large number of small coolant passages near the airfoil surface. A method of satisfactorily removing the small ceramic cores which formed the cooling passages in the casting process was also developed.

2. The cast-cored blade showed substantial reduction from the effective gas temperature over the entire range of coolant-to-gas flow ratios investigated in the central part of the highly stressed root region. For example, a 520° reduction from effective gas temperature was observed in this region at rated engine operating conditions and a coolant-to-gas flow ratio of 0.010.

3. A total of 78 hours of endurance operation without failure was obtained with one of the test blades at a centrifugal blade stress of 42,150 pounds per square inch based on total metal area at the blade root at rated engine speed and an average inlet gas temperature of 1735° F. Of this total, 50 hours were obtained with an average blade root metal temperature of 883° F (coolant-to-gas flow ratio of 0.015) and 28 hours with an average blade root metal temperature of 1130° F (coolant-to-gas flow ratio of 0.004).

4. Calculations indicate that this blade would require a ratio of coolant-to-gas flow of approximately 0.023 to maintain an average root temperature of 883° F, assuming the blade to be employed in a turbojet engine at an inlet gas temperature of 2000° F, an altitude of 50,000 feet, and a Mach number of 2.

5. Cast-cored blade weight (0.82 lb) was approximately the same as that of a standard uncooled blade for this engine. At least a 13-percent reduction from the standard uncooled blade weight appeared possible by combining cast-cored and hollow-blade designs.

Lewis Flight Propulsion Laboratory
National Advisory Committee for Aeronautics
Cleveland, Ohio, March 7, 1956

APPENDIX - SYMBOLS

c_p specific heat at constant pressure, Btu/(lb)(°F)

g acceleration due to gravity, 32.2 ft/sec^2

h heat-transfer coefficient, Btu/(hr)(ft^2)(°F)

J mechanical equivalent of heat, 778 ft-lb/Btu

j chordwise distance from trailing edge to blade cooling passage, ft

k thermal conductivity, Btu/(hr)(ft)(°F)

l perimeter, ft

r radius, ft

T temperature, °F

ΔT temperature change in differential element Δz along span, °F

w weight flow, lb/sec

y distance from trailing edge to blade element, ft

z distance from blade root to span position being considered, ft

Δz differential element along blade span, ft

θ temperature difference, $T_{g,e} - T_B$

τ thickness of trailing section, ft

φ $(2h_o/k_B\tau)^{1/2}$

ω angular velocity of turbine wheel, radians/sec

Subscripts:

a blade cooling air

B cooled blade

e effective

g combustion gas

i inside (coolant side)

l perimeter

o outside (on gas side)

r root of blade

Superscripts:

' linear dimension increased by $\tau/2$

— average value within spanwise increment being considered

REFERENCES

1. Ellerbrock, Herman H., Jr., and Stepka, Francis S.: Experimental Investigation of Air-Cooled Turbine Blades in Turbojet Engine. I - Rotor Blades with 10 Tubes in Cooling-Air Passages. NACA RM E50I04, 1950.

2. Hickel, Robert O., and Ellerbrock, Herman H., Jr.: Experimental Investigation of Air-Cooled Turbine Blades in Turbojet Engine. II - Rotor Blades with 15 Fins in Cooling-Air Passages. NACA RM E50I14, 1950.

3. Hickel, Robert O., and Smith, Gordon T.: Experimental Investigation of Air-Cooled Turbine Blades in Turbojet Engine. III - Rotor Blades with 34 Steel Tubes in Cooling-Air Passages. NACA RM E50J06, 1950.

4. Ellerbrock, Herman H., Jr., Zalabak, Charles F., and Smith, Gordon T.: Experimental Investigation of Air-Cooled Turbine Blades in Turbojet Engine. IV - Effects of Special Leading- and Trailing-Edge Modifications on Blade Temperature. NACA RM E51A19, 1951.

5. Smith, Gordon T., and Hickel, Robert O.: Experimental Investigation of Air-Cooled Turbine Blades in Turbojet Engine. V - Rotor Blades with Split Trailing Edges. NACA RM E51A22, 1951.

6. Arne, Vernon L., and Esgar, Jack B.: Experimental Investigation of Air-Cooled Turbine Blades in Turbojet Engine. VI - Conduction and Film Cooling of Leading and Trailing Edges of Rotor Blades. NACA RM E51C29, 1951.

7. Smith, Gordon T., and Hickel, Robert O.: Experimental Investigation of Air-Cooled Turbine Blades in Turbojet Engine. VIII - Rotor Blades with Capped Leading Edges. NACA RM E51H14, 1951.

8. Stepka, Francis S., and Hickel, Robert O.: Experimental Investigation of Air-Cooled Turbine Blades in Turbojet Engine. IX - Evaluation of the Durability of Noncritical Rotor Blades in Engine Operation. NACA RM E51J10, 1951.

9. Esgar, Jack B., and Clure, John L.: Experimental Investigation of Air-Cooled Turbine Blades in Turbojet Engine. X - Endurance Evaluation of Several Tube-Filled Rotor Blades. NACA RM E52B13, 1952.

10. Bartoo, Edward R., and Clure, John L.: Experimental Investigation of Air-Cooled Turbine Blades in Turbojet Engine. XII - Cooling Effectiveness of a Blade with an Insert and with Fins Made of a Continuous Corrugated Sheet. NACA RM E52F24, 1952.

11. Stepka, Francis S., Bear, H. Robert, and Clure, John L.: Experimental Investigation of Air-Cooled Turbine Blades in Turbojet Engine. XIV - Endurance Evaluation of Shell-Supported Turbine Rotor Blades Made of Timken 17-22A(S) Steel. NACA RM E54F23a, 1954.

12. Schum, Eugene F., Stepka, Francis S., and Oldrieve, Robert E.: Fabrication and Endurance of Air-Cooled Strut-Supported Turbine Blades with Struts Cast of X-40 Alloy. NACA RM E56A12, 1956.

13. Long, Roger A., and Esgar, Jack B.: Experimental Investigation of Air-Cooled Turbine Blades in Turbojet Engine. VII - Rotor-Blade Fabrication Procedures. NACA RM E51E23, 1951.

14. Glenny, E.: The Application of the Investment-Casting Technique to the Manufacture of Blade Shapes Containing Cooling Fluid Passages. Memo. No. M.122, British N.G.T.E., Dec. 1951.

15. Ellerbrock, Herman H., Jr., Schum, Eugene F., and Nachtigall, Alfred J.: Use of Electric Analogs for Calculation of Temperature Distribution of Cooled Turbine Blades. NACA TN 3060, 1953.

16. Hubbartt, James E., and Schum, Eugene F.: Average Outside-Surface Heat-Transfer Coefficients and Velocity Distributions for Heated and Cooled Impulse Turbine Blades in Static Cascades. NACA RM E50L20, 1951.

17. Brown, W. Bryon, and Donoughe, Patrick L.: Extension of Boundary-Layer Heat-Transfer Theory of Cooled Turbine Blades. NACA RM E50F02, 1950.

18. Slone, Henry O., Hubbartt, James E., and Arne, Vernon L.: Method of Designing Corrugated Surfaces Having Maximum Cooling Effectiveness Within Pressure-Drop Limitations for Application to Cooled Turbine Blades. NACA RM E54H20, 1954.

19. Livingood, John N. B., and Brown, W. Bryon.: Analysis of Temperature Distribution in Liquid-Cooled Turbine Blades. NACA TN 2321, 1951.

20. Schum, Eugene F.: Additional Experimental Heat-Transfer and Durability Data on Several Forced-Convection, Air-Cooled, Strut-Supported Turbine Blades of Improved Design. NACA RM E54J25, 1955.

21. Slone, Henry O., and Hubbartt, James E.: Analysis of Factors Affecting Selection and Design of Air-Cooled Single-Stage Turbines for Turbojet Engines. IV - Coolant-Flow Requirements and Performance of Engines Using Air-Cooled Corrugated-Insert Blades. NACA RM E55C09, 1955.

22. Slone, Henry O., and Esgar, Jack B.: Gas-to-Blade Heat-Transfer Coefficients and Turbine Heat-Rejection Rates for a Range of One-Spool Turbine Engine Designs. NACA RM E56A31, 1956.

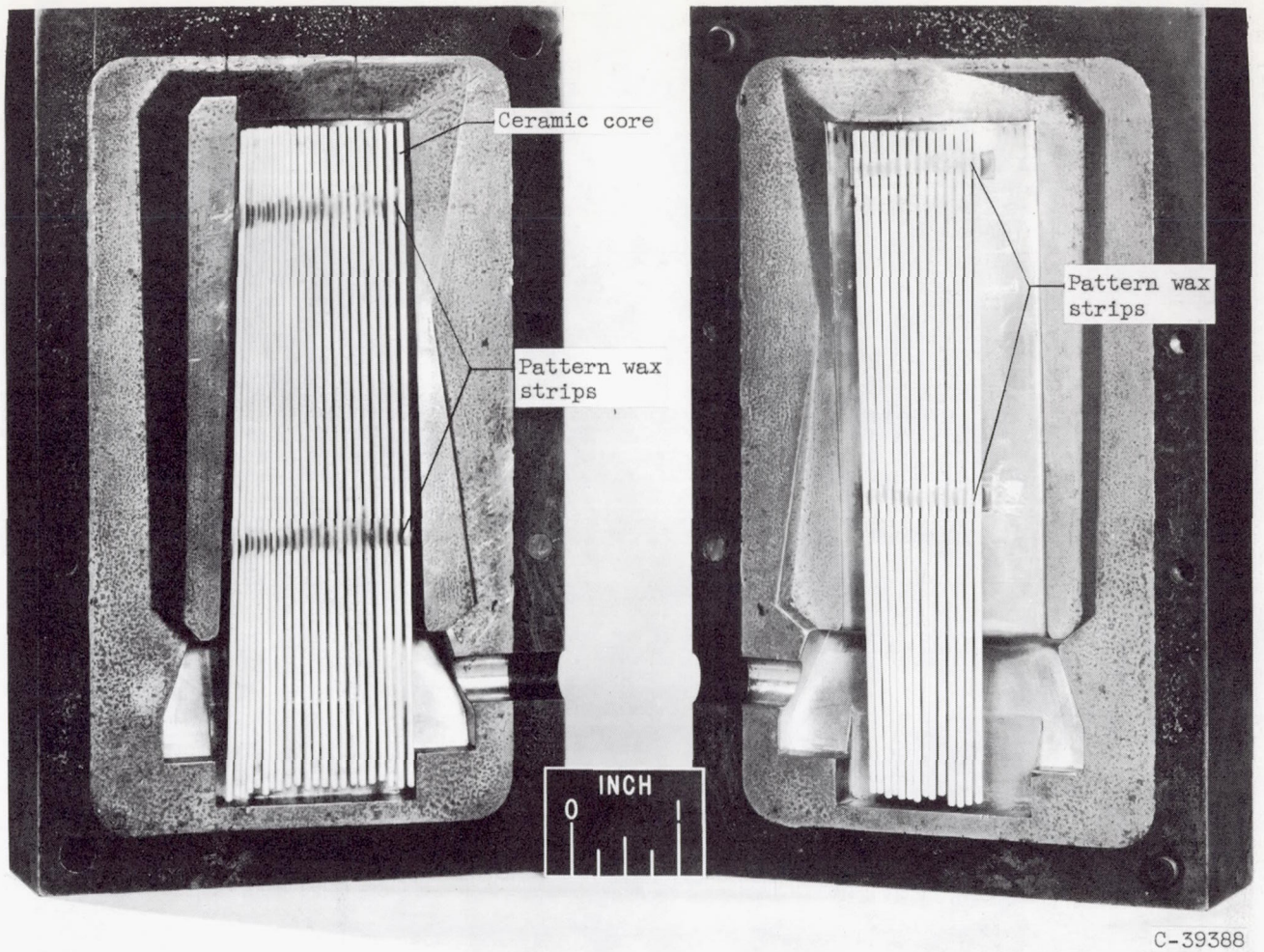

Suction-surface die

Pressure-surface die

Figure 1. - Die halves showing stage of ceramic-core assembly.

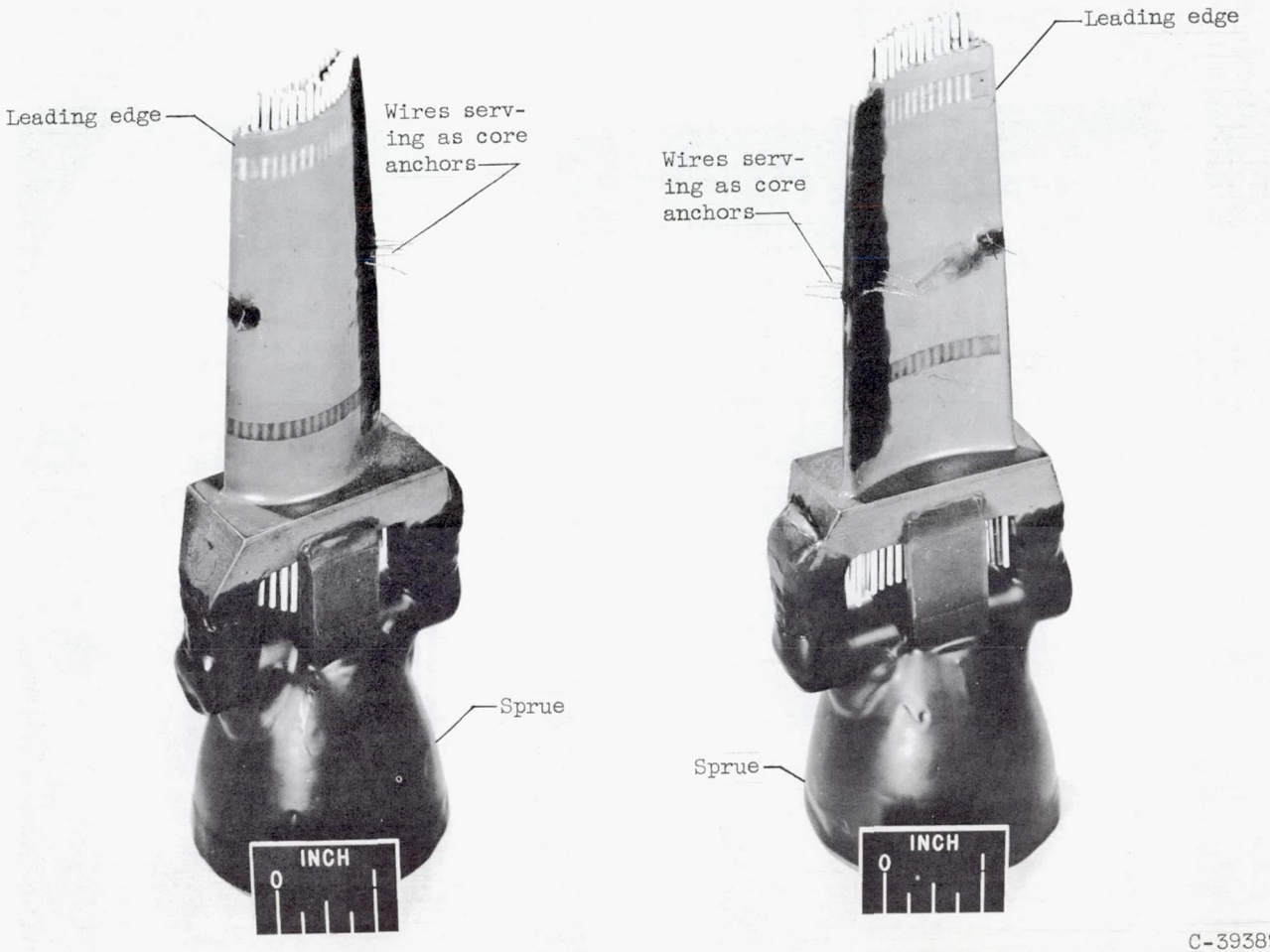

Figure 2. - Completed wax pattern attached to wax sprue.

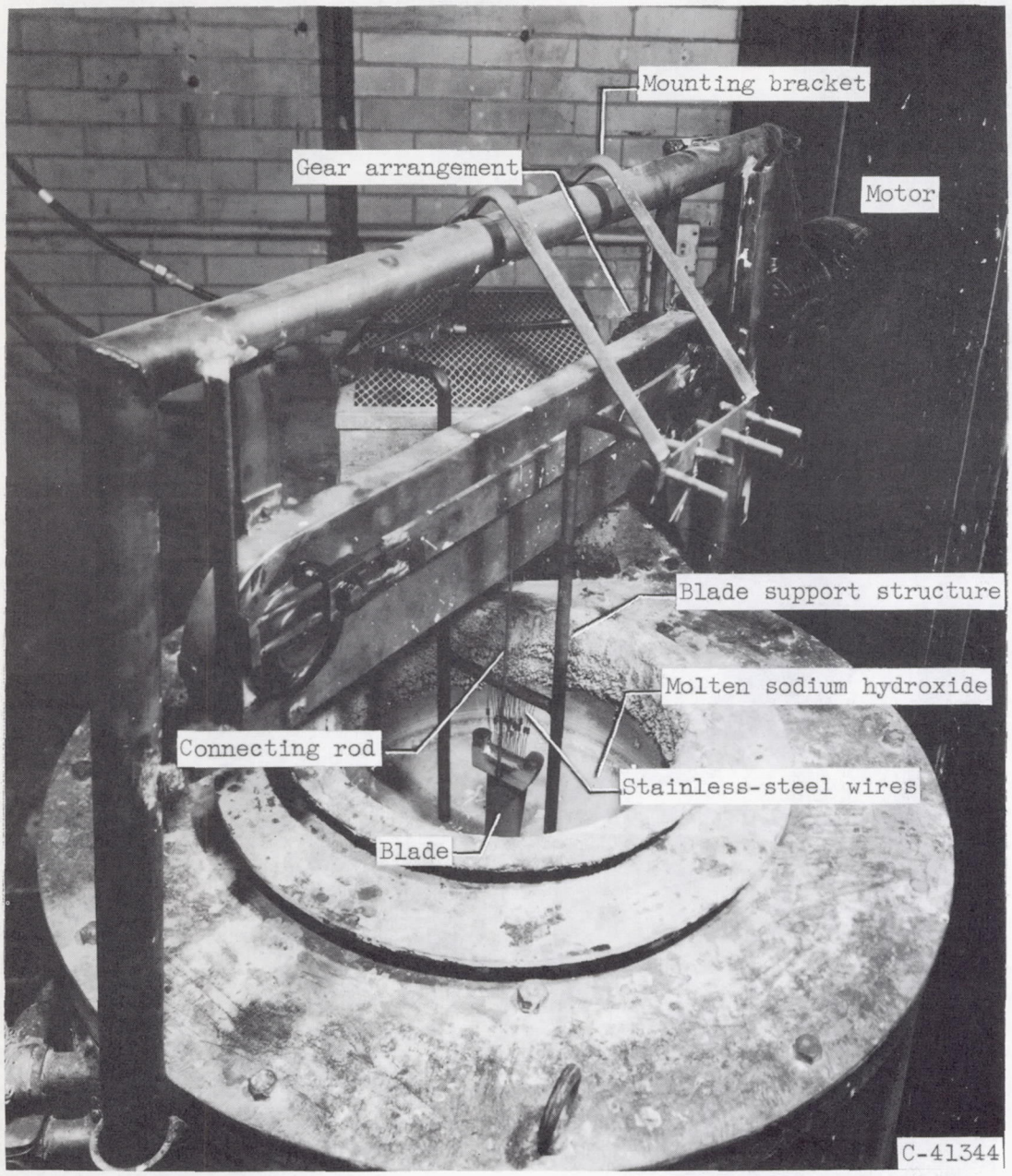

Figure 3. - Cast-cored blade in core removal device.

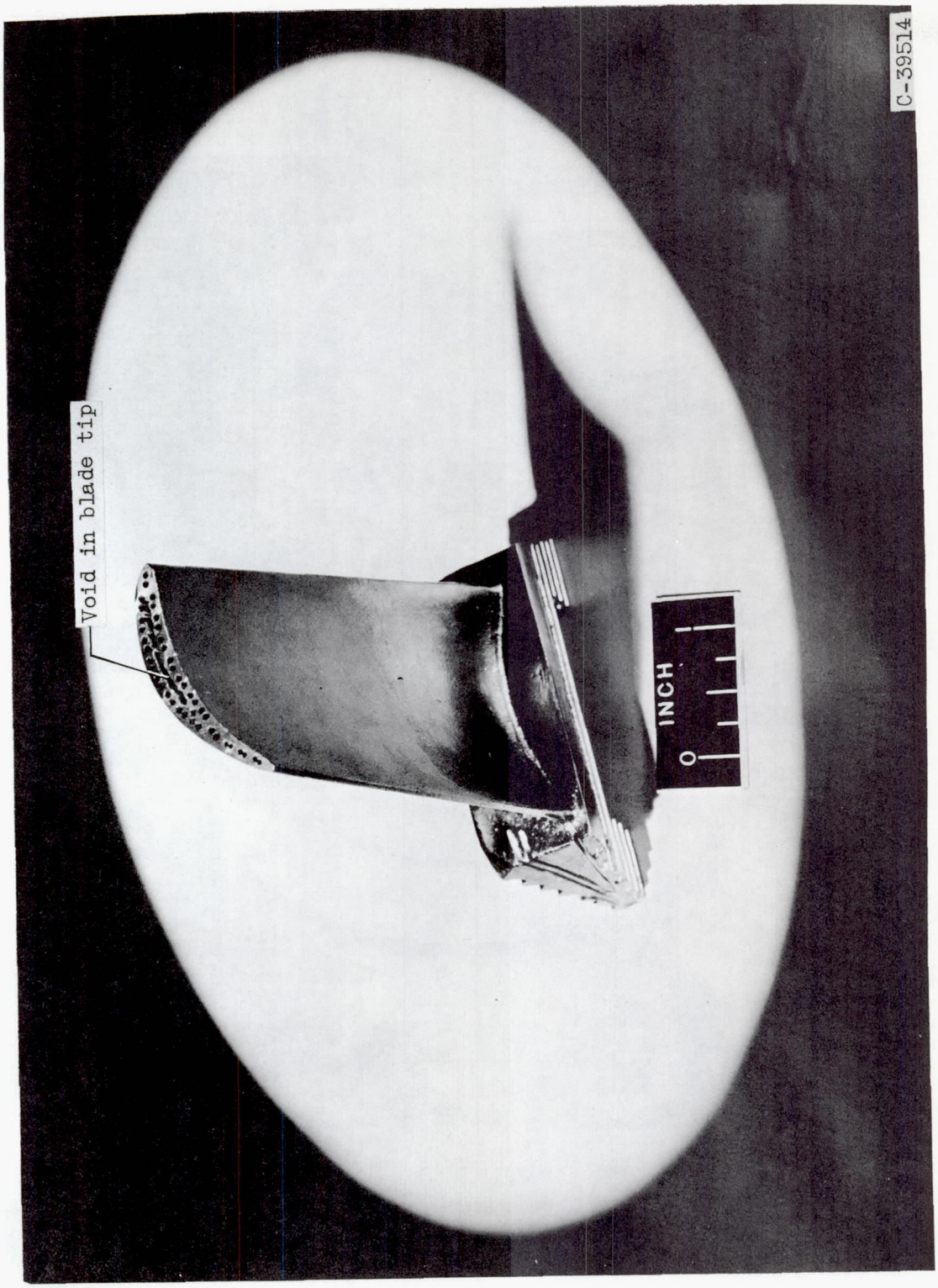

Figure 4. - Test blade.

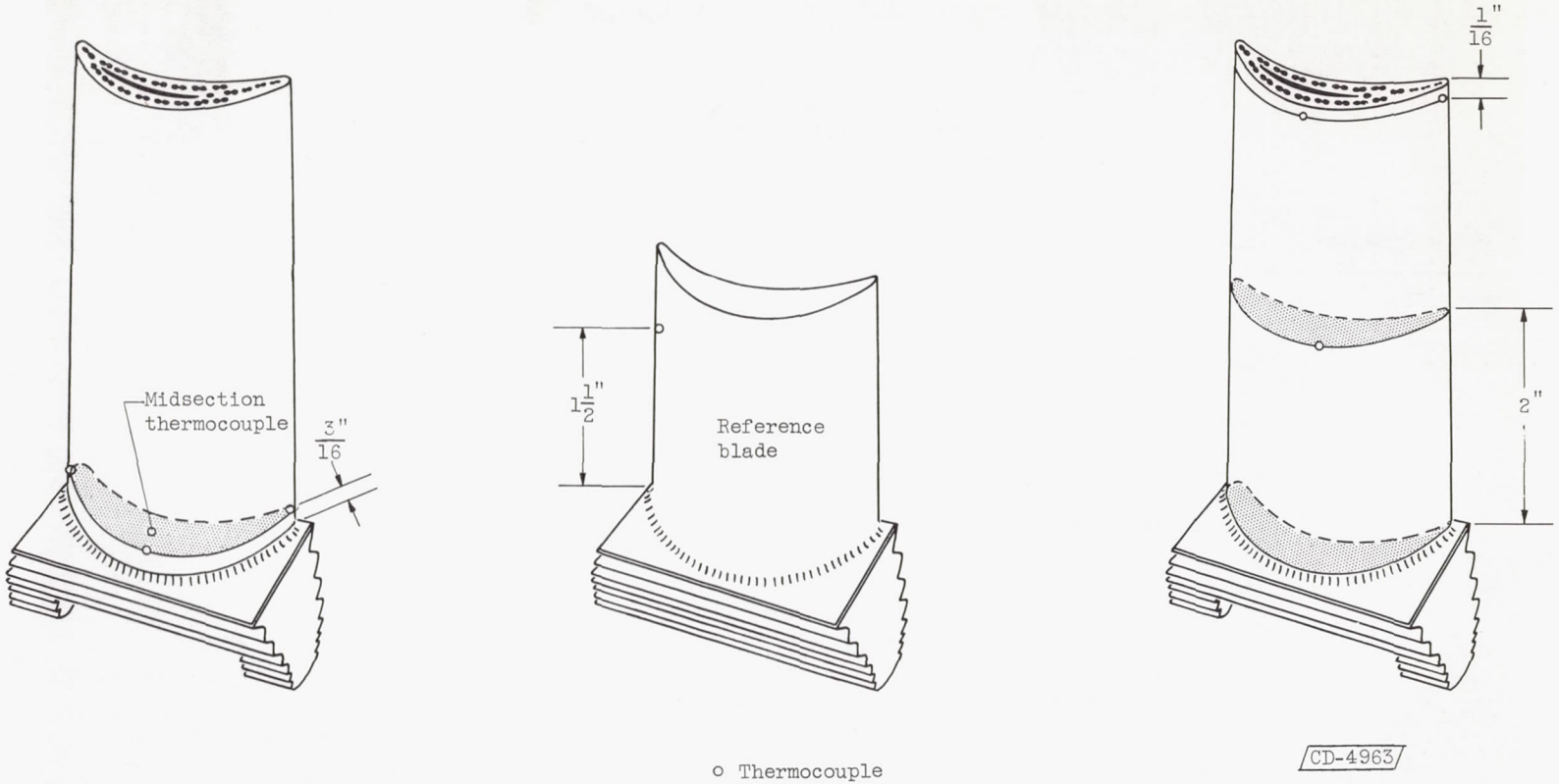

Figure 5. - Thermocouple installation on cooled and uncooled blades.

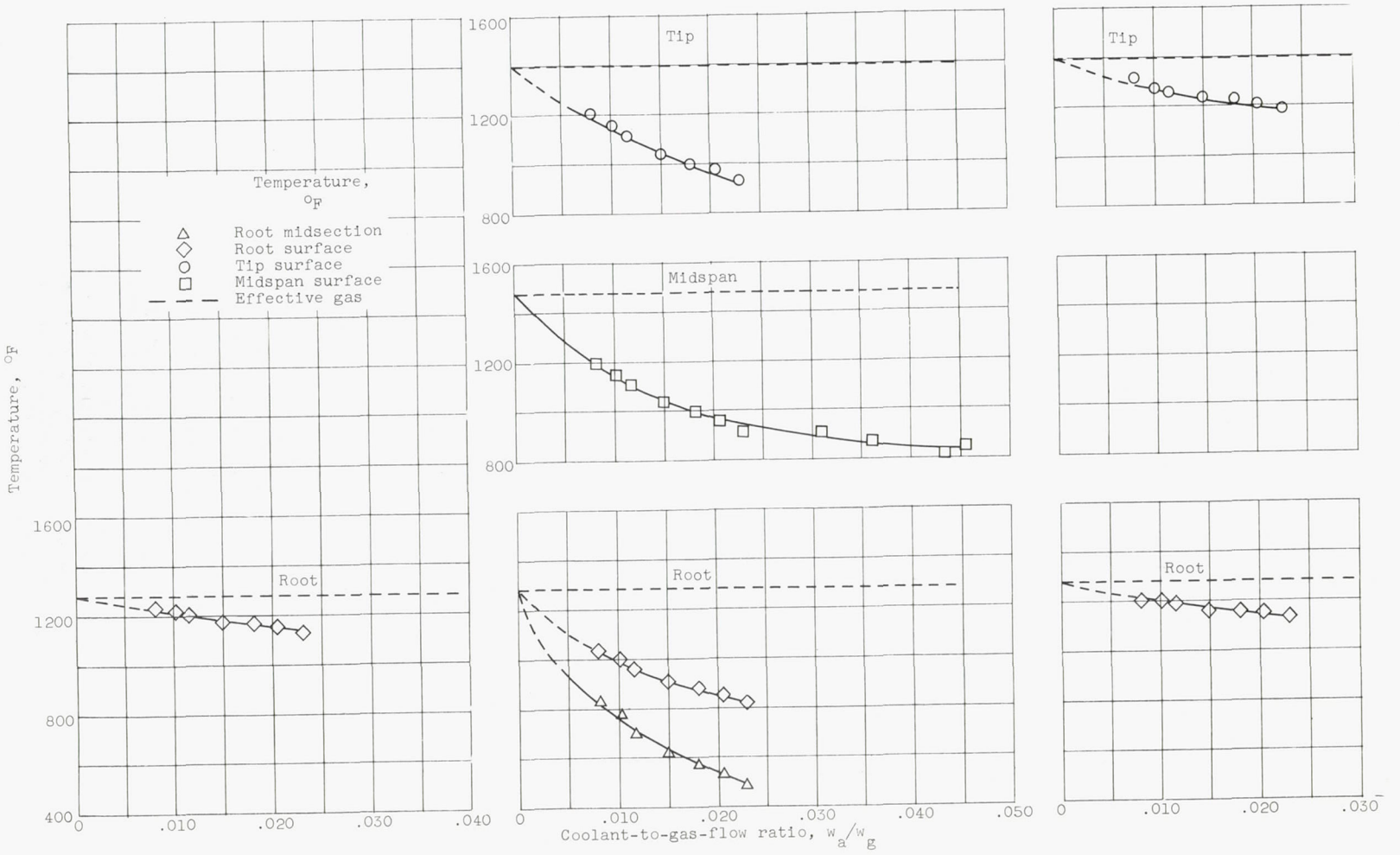

(a) Leading edge. (b) Midchord. (c) Trailing edge.

Figure 6. - Variation of air-cooled cast-cored blade temperatures with coolant-to-gas flow ratio at rated engine speed.

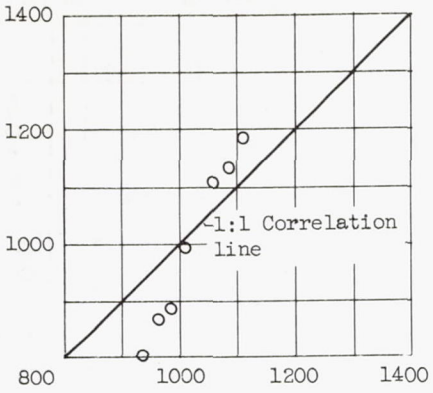

(a) Average root surface temperature.

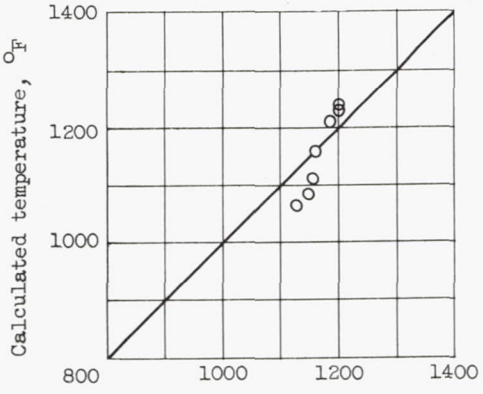

(b) Root trailing-edge temperature.

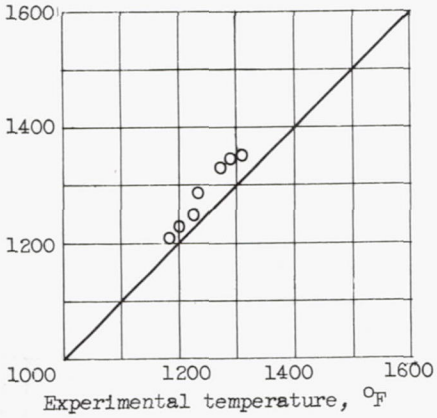

(c) Tip trailing-edge temperature.

Figure 7. - Comparison of calculated with experimental temperatures for the cast-cored blade over coolant-to-gas-flow-ratio range of 0.008 to 0.023 at rated engine speed and inlet gas temperature of 1725° F.

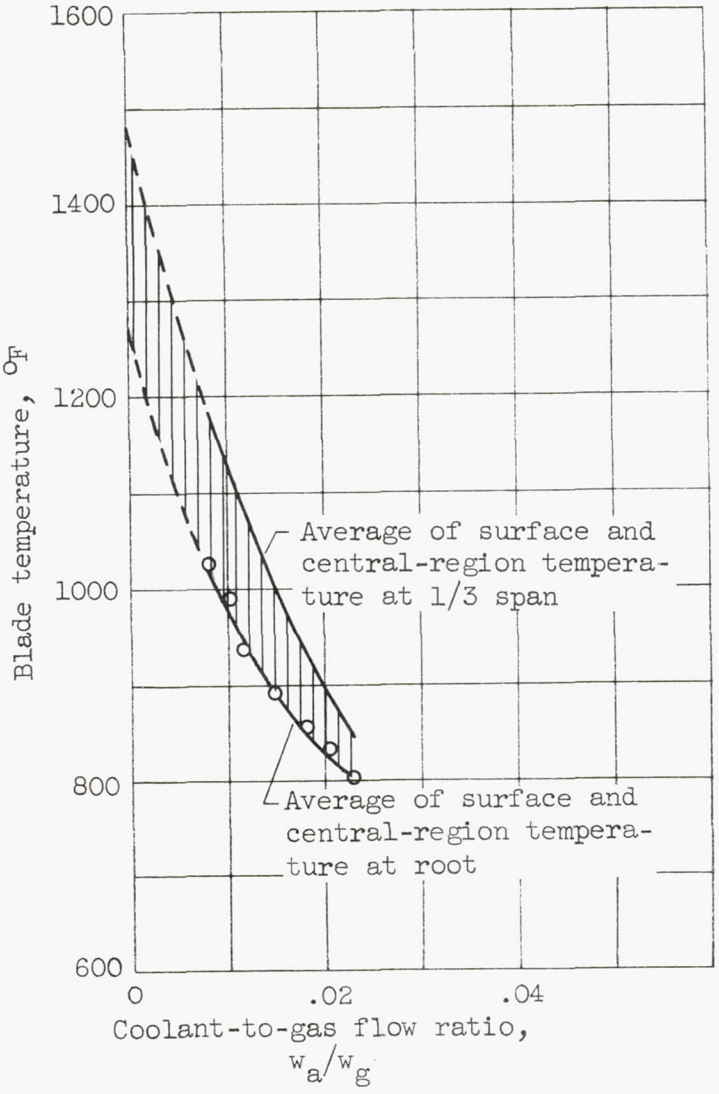

Figure 8. - Change in average blade temperatures with coolant-to-gas-flow ratio at root and 1/3-span position for rated engine speed and turbine-inlet gas temperatures ranging from 1655° to 1725° F.

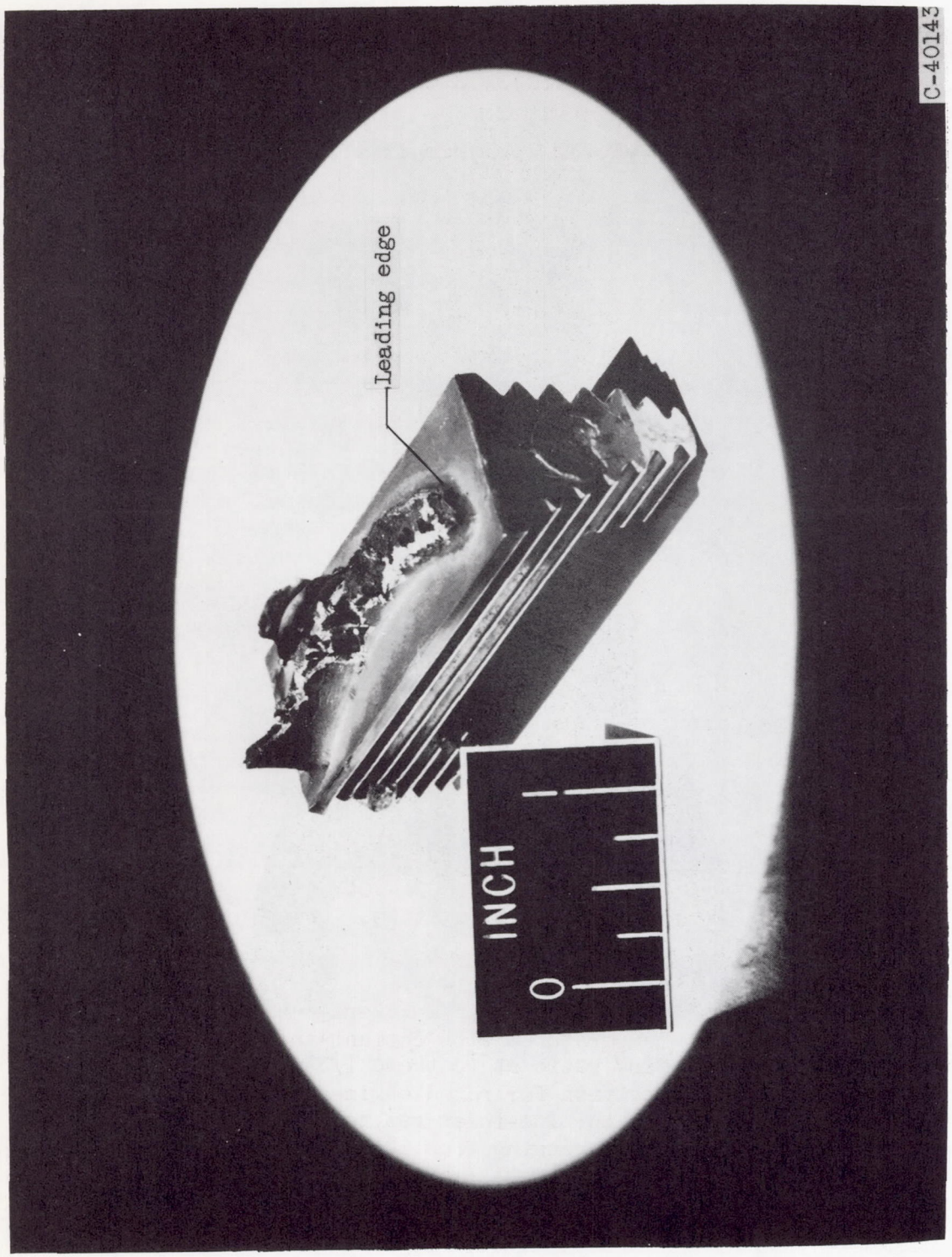

Figure 9. - Failed blade.

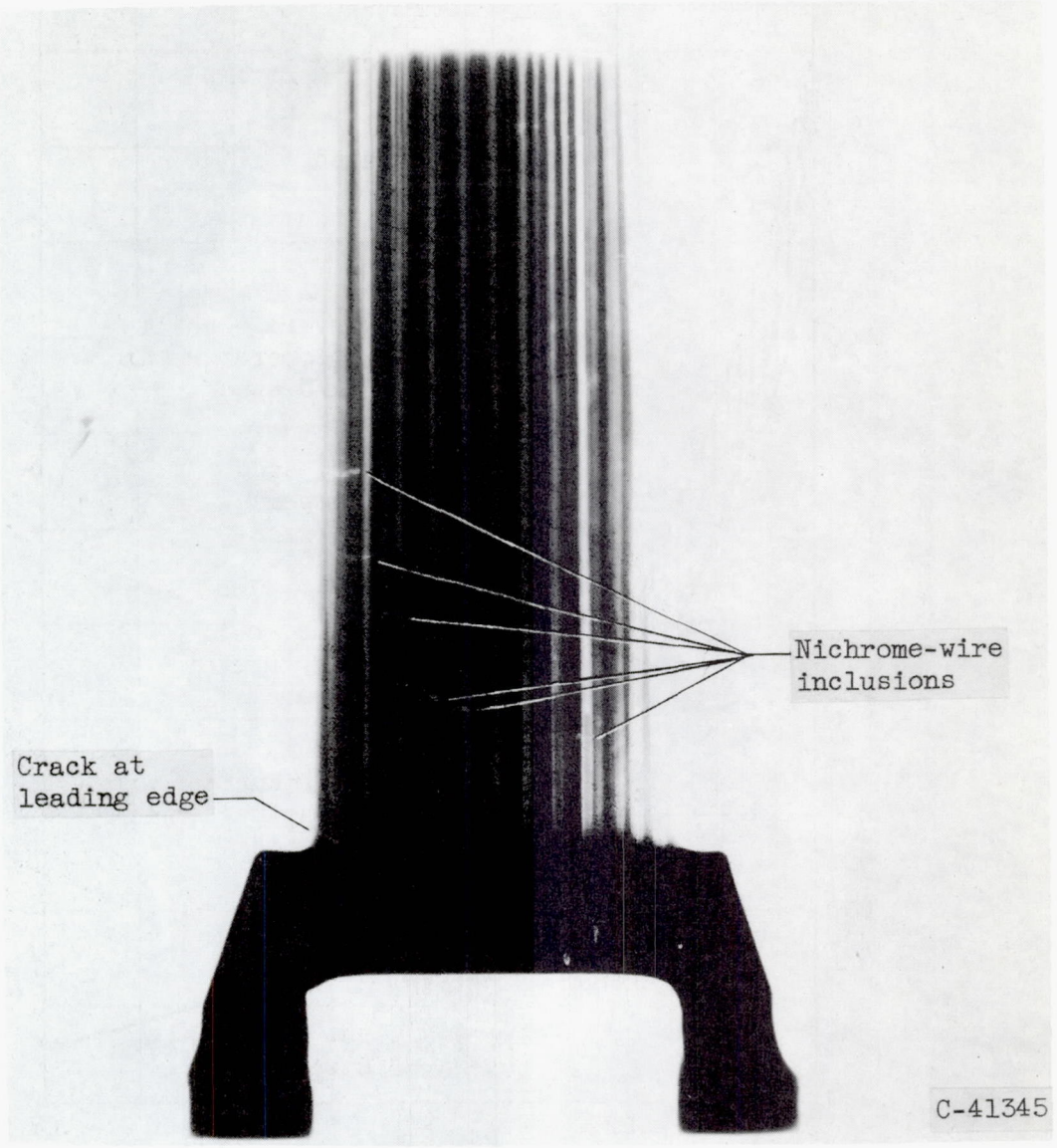

Figure 10. - X-ray of final casting showing casting defects.

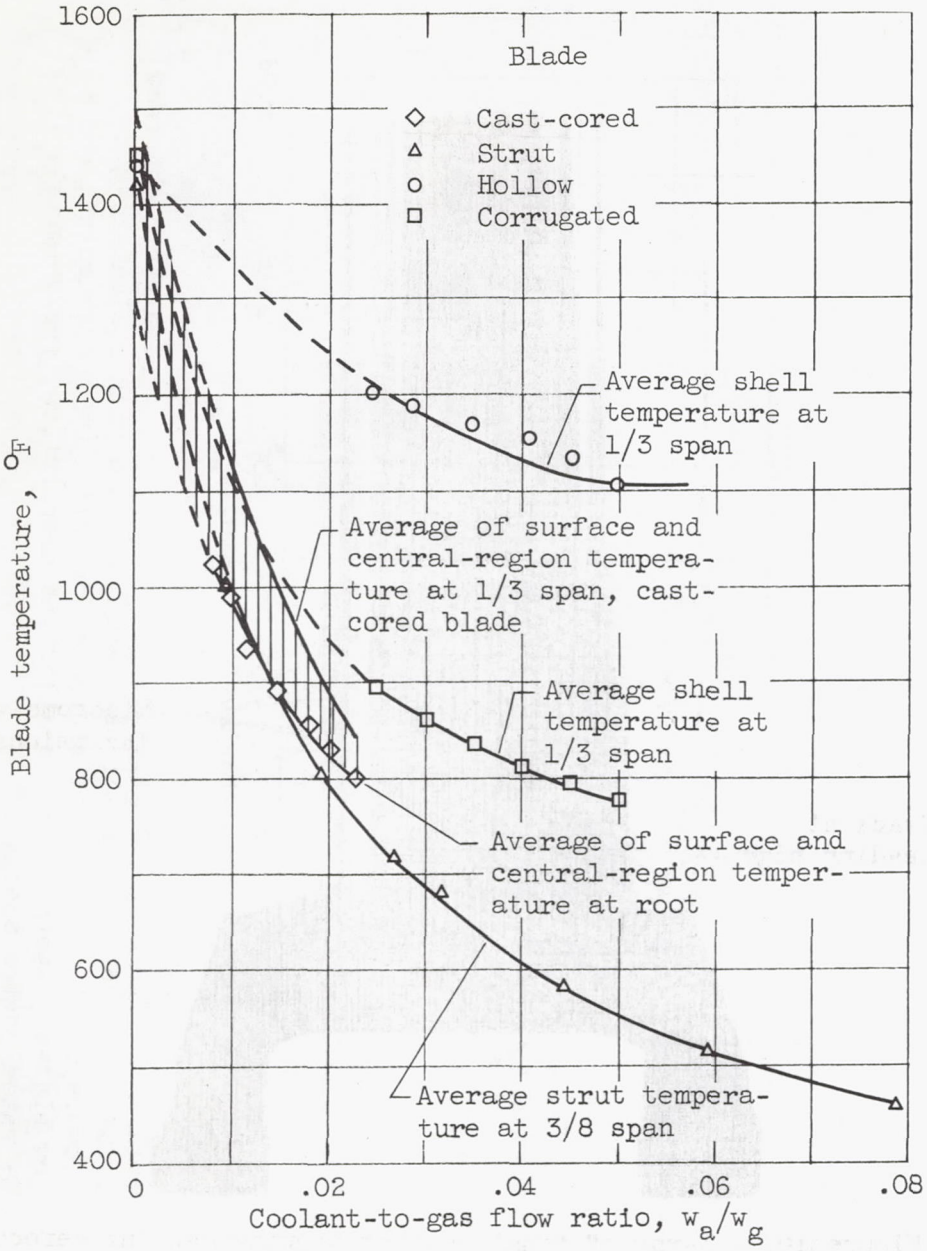

Figure 11. - Blade temperature comparison of cast-cored blade and other blade configurations at the critical sections for rated engine speed and turbine-inlet gas temperatures ranging from 1655° to 1725° F.

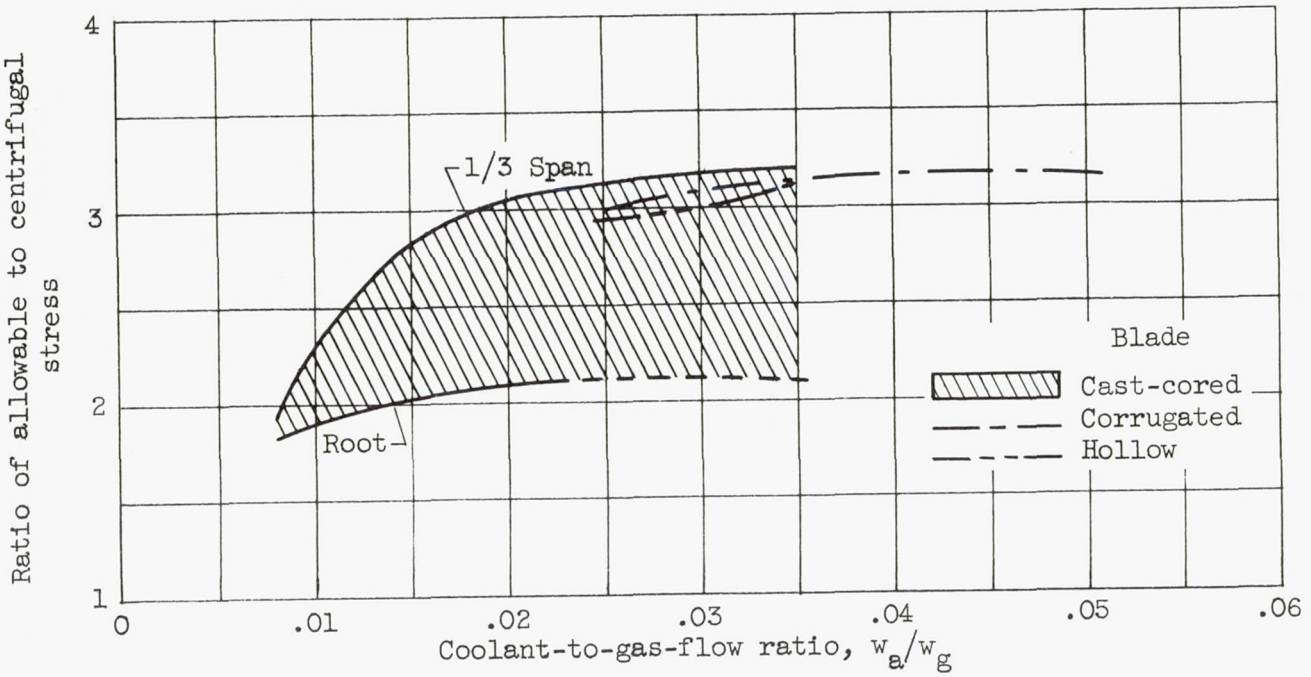

Figure 12. - Variation of allowable-to-centrifugal-stress ratio obtained from yield and 100-hour stress-to-rupture data with coolant-to-gas-flow ratio at the critical sections for cast-cored, corrugated, and hollow blades. Average turbine-inlet gas temperature, approximately 1690° F; rated engine speed.

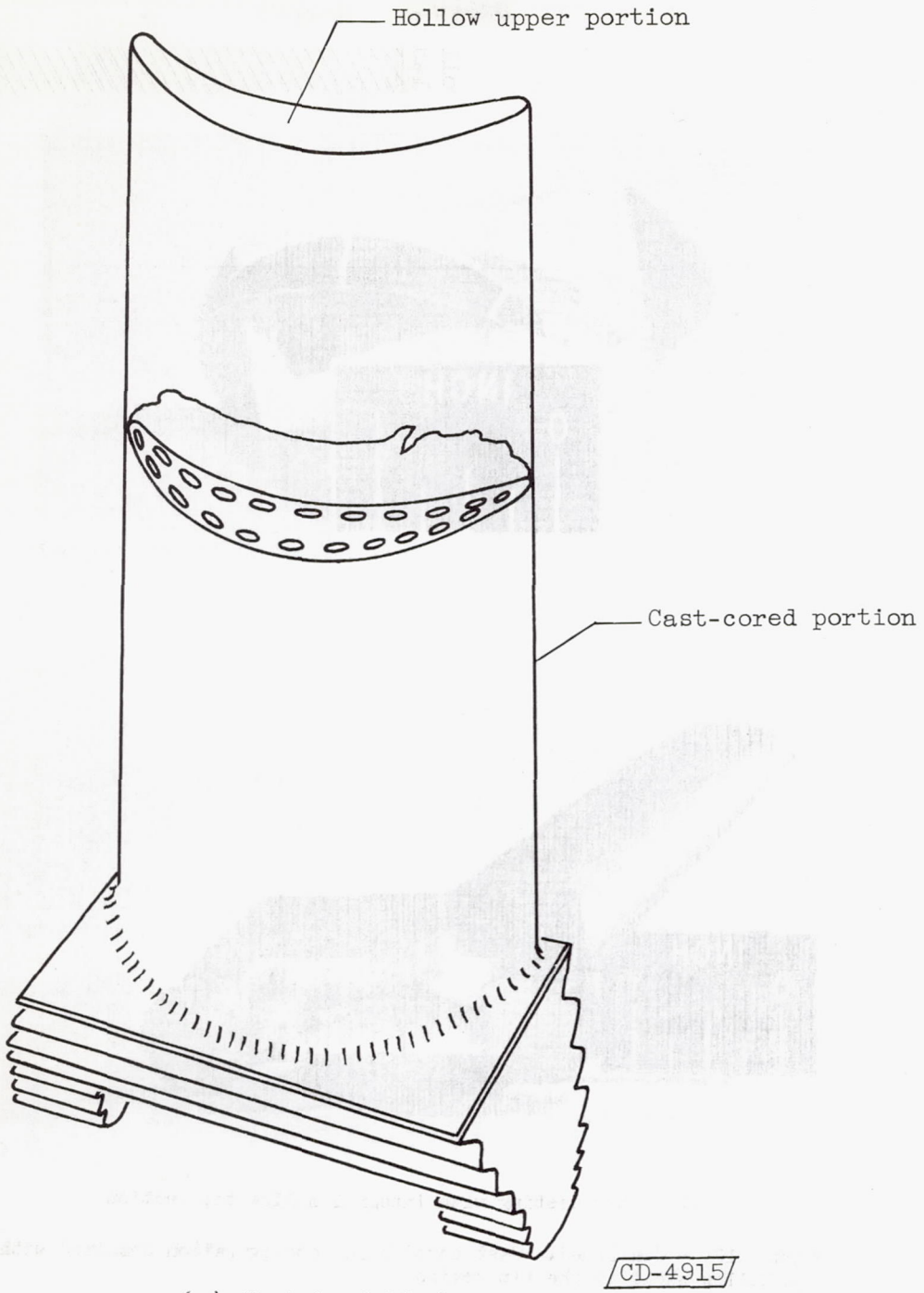

(a) Sketch of blade.

Figure 13. - Cast-cored blade configuration combined with a hollow shell in the tip region.

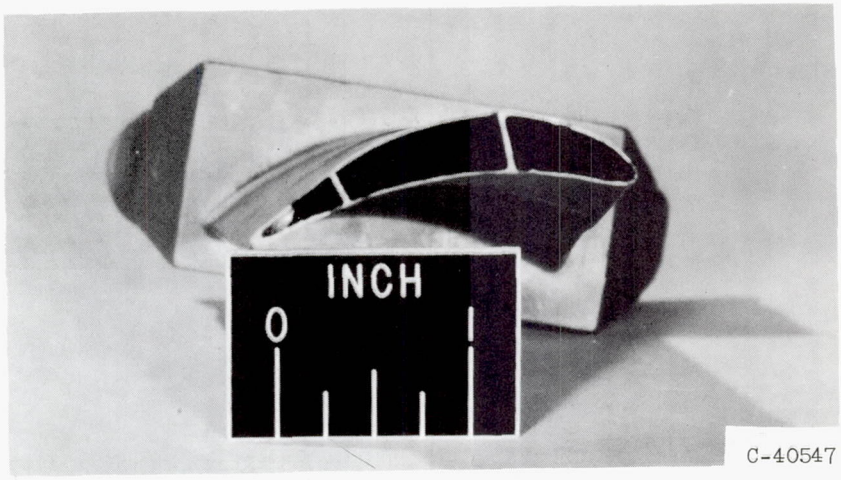

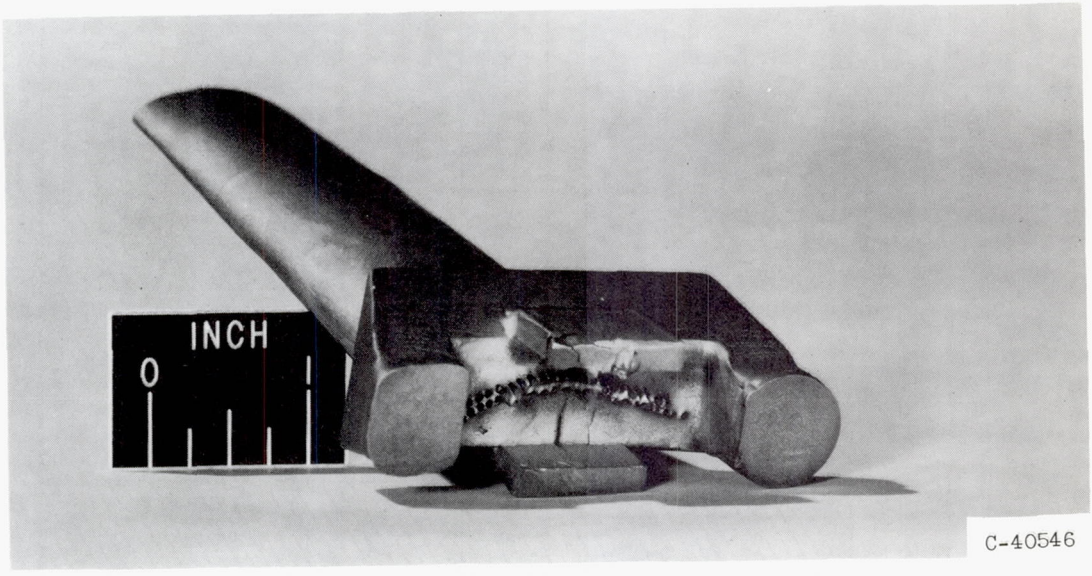

(b) Blade casting with integral hollow tip section.

Figure 13. - Concluded. Cast-cored blade configuration combined with a hollow shell in the tip region.

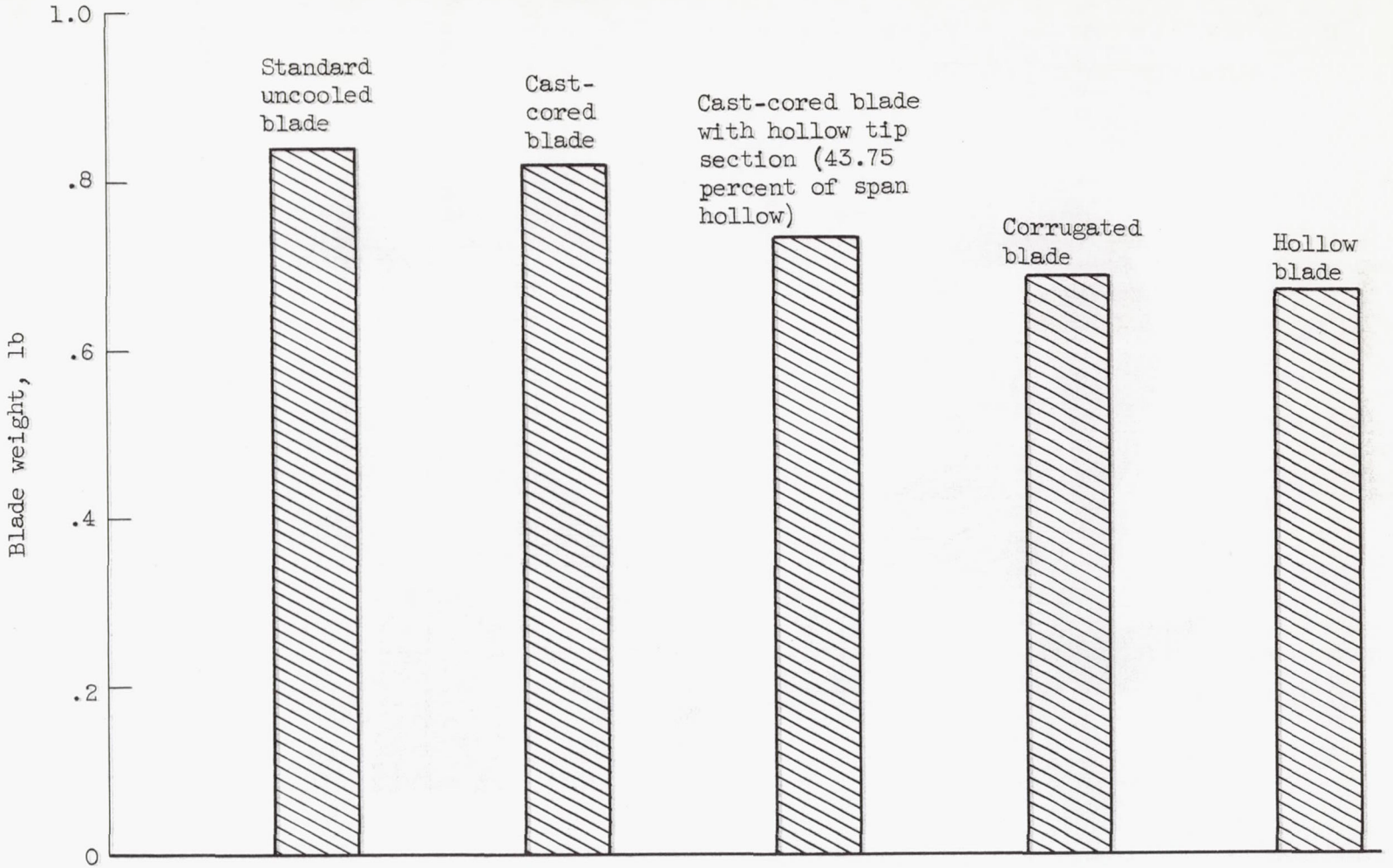

Figure 14. - Blade weight comparisons.